VA1213, a selective COX-2 inhibitor, exhibits antitumor activity by suppressing EGFR, AKT, and ERK1/2 phosphorylation

VA1213, a selective COX-2 inhibitor, exhibits antitumor activity by suppressing EGFR, AKT, and ERK1/2 phosphorylation

Valerio Ciccone , Claudia Cecchin , Maria Frosini , Mario Saletti , Samuele Maramai , Germano Giuliani , Marco Paolino , Andrea Cappelli , Maurizio Anzini , Sandra Donnini , Lucia Morbidelli

PII: S0928-0987(25)00419-1
DOI: https://doi.org/10.1016/j.ejps.2025.107422
Reference: PHASCI 107422

To appear in: *European Journal of Pharmaceutical Sciences*

Received date: 22 July 2025
Revised date: 5 December 2025
Accepted date: 20 December 2025

Please cite this article as: Valerio Ciccone , Claudia Cecchin , Maria Frosini , Mario Saletti , Samuele Maramai , Germano Giuliani , Marco Paolino , Andrea Cappelli , Maurizio Anzini , Sandra Donnini , Lucia Morbidelli , VA1213, a selective COX-2 inhibitor, exhibits antitumor activity by suppressing EGFR, AKT, and ERK1/2 phosphorylation, *European Journal of Pharmaceutical Sciences* (2025), doi: https://doi.org/10.1016/j.ejps.2025.107422

VA1213, a selective COX-2 inhibitor, exhibits antitumor activity by suppressing EGFR, AKT, and ERK1/2 phosphorylation

Valerio Ciccone[1], Claudia Cecchin[1], Maria Frosini[1], Mario Saletti[2], Samuele Maramai[2], Germano Giuliani[2], Marco Paolino[2], Andrea Cappelli[2], Maurizio Anzini[2], Sandra Donnini[1], Lucia Morbidelli[1,*]

[1]Department of Life Sciences, University of Siena, Siena I-53100, Italy
[2]Department of Biotechnology, Chemistry and Pharmacy, University of Siena, Siena I-53100, Italy

*Correspondence to: Prof. Lucia Morbidelli, Department of Life Sciences, University of Siena, Via Aldo Moro 2, 53100 Siena, Italy email: lucia.morbidelli@unisi.it

Keywords: COX-2, antitumor activity, nonsteroidal anti-inflammatory drugs, colorectal cancer

Graphical Abstract

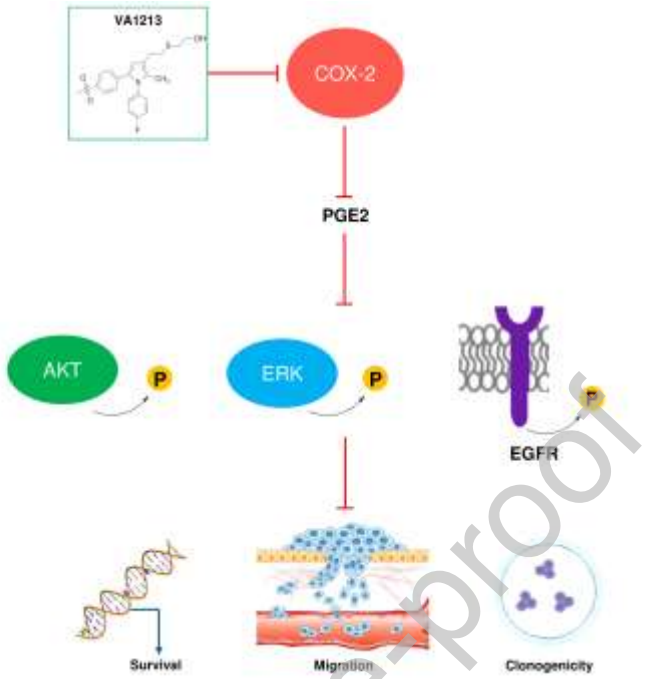

Abstract

Cyclooxygenase-2 (COX-2) is overexpressed in various cancers and has emerged as a promising target in oncological pharmacotherapy.

This study investigates the *in vitro* antitumor properties and mechanism of action of novel vicinal diaryl-substituted heterocyclic COX-2 inhibitors, with a focus on **VA1213**, in comparison to celecoxib, a widely marketed COX-2 inhibitor known for its off-target effects. We assessed cytotoxicity, apoptosis induction, cell-cycle distribution, antimetastatic activity, and alterations in key signaling pathways in HT-29 colorectal carcinoma and MDA-MB-231 breast carcinoma cell lines. Among the novel compounds, **VA1213** exhibited the most potent growth-inhibitory activity, demonstrating time-dependent cytotoxicity with a lower IC_{50} after 48–72 hours of treatment compared to **VA692** and **VA694**, and consistent with that observed for celecoxib.

Unlike celecoxib, which produced rapid cytotoxic effects, **VA1213** required prolonged exposure, suggesting a distinct mechanism of action. **VA1213** induced G_0/G_1 phase cell cycle arrest and apoptosis via caspase-3 activation. Furthermore, it impaired EGFR downstream signaling by reducing ERK1/2 and AKT phosphorylation, without directly inhibiting EGFR itself. At sub-cytotoxic concentrations, **VA1213** was more effective than celecoxib in inhibiting cell migration and demonstrated a comparable reduction in clonogenic potential. These findings highlight **VA1213** as a COX-2 inhibitor with noteworthy *in vitro* antitumor efficacy, comparable to that of celecoxib. Its ability to interfere with multiple cancer-associated signaling pathways and reduce tumor cell aggressiveness underscores its potential as a promising therapeutic candidate. Further *in vivo* studies are warranted to confirm its efficacy and assess potential off-target effects.

1. Introduction

Cyclooxygenases (COX) are crucial enzymes that catalyze the conversion of arachidonic acid into prostaglandins, existing in two main isozymes: COX-1 and COX-2. COX-1 is constitutively expressed in various normal tissues, whereas COX-2 is inducible and often overexpressed in inflammatory conditions as well as in many types of neoplastic tissues [1–3]. Among the products of COX-2, prostaglandin E2 (PGE2) is a lipid mediator that supports epithelial tumor aggressiveness by several mechanisms, including growth promotion, escape from apoptosis, transactivation of tyrosine kinase growth factor receptors, and induction of angiogenesis [4,5].

COX-2 overexpression has been implicated in the pathogenesis of several cancers, including colorectal cancer (CRC) and triple-negative breast cancer (TNBC). The role of COX-2 derived mediators in carcinogenesis and progression of these tumors has been well-documented over several years [6–10].

Traditional NSAIDs exert clinical efficacy mainly through COX-2 inhibition, modulating pain, fever, inflammation, tumorigenesis, and cancer progression [11–13]. Selective COX-2 inhibitors, or coxibs, retain anti-inflammatory effects while reducing gastrointestinal toxicity. They also suppress tumor growth and induce apoptosis in colorectal cancer cells by targeting pathways like PI3K/AKT and MAPK/ERK [14,15]. Celecoxib, the first FDA-approved coxib (December 1998), marketed as Celebrex®, shares class-associated dose-dependent cardiovascular risks [16]. Moreover, over 44 off-target proteins have been identified for celecoxib, underscoring the need for better-tolerated COX-2 inhibitors [17]. Future efforts should focus on designing more selective, better-tolerated inhibitors.

In the last decade, the synthesis of hybrid structures endowed with selective COX-2 inhibitory properties while also capable to release nitric oxide (NO) (NO-donors), also known as CINOD [18], has prompted the development of new anti-inflammatory and antinociceptive drugs. These agents were specifically designed with the aim of avoiding cardiovascular and renal side effects, particularly those related to the use of vicinal diaryl-substituted heterocycles (VDHs), to which coxibs structurally belong [18].

With two phenyl rings on adjacent atoms of a five- or six-membered heterocyclic system, VDHs are a family of privileged scaffolds that have recently attracted considerable attention in correlation to their potential clinical applications [19]. In light of this, we carried out a thorough investigation into the development of 3-substituted-1,5-diarylpyrrole derivatives. These latter include carboxylic acids and esters [20], alkoxy ethers [21,22], alkyl sulfides and sulfoxides [23] along with NO-releasing moieties such as nitrooxyalkyl esters, [24] and ethers (e. g. **VA694**) [20,21,23–25] evaluated for their anti-inflammatory and selective COX-2 inhibitory activities. The vast majority of these compounds demonstrated potent biological activities in *in vitro*, *in vivo*, and *ex vivo* studies, comparable to those of the standard COX-2 inhibitors (e.g. celecoxib) [25]. The discovery of nitrooxy analogs [24] paved the way for the development of novel dual COX-2 inhibitors/NO donors with NO-dependent vasorelaxant property [26], therefore promoting gastrointestinal and cardiovascular safety. Both nitrooxyalkyl inverse ethers and their metabolites, hydroxyethyl derivatives (e. g. **VA692**) displayed very potent COX-2 inhibitory activity in the nanomolar range [25,27]. Spurred by the encouraging results of previously reported nitrooxy- and hydroxyethyl ethers [25], we concentrated on the synthesis of nitrooxy- and hydroxy ethyl sulfides (e.g., **VA1213**) as thio-analogs of **VA694** and **VA692**, as well as their oxidation products, nitrooxy- and hydroxyethyl sulfoxides, respectively (also referred to as thio-CINOD) [28]. In fact, the replacement of oxygen to sulfur atom is a well-established bioisosteric substitution frequently adopted in medicinal chemistry [23]. Specifically, sulfur-containing homologues contributed to expanding structure activity relationship studies and demonstrated favorable interactions within COX-2 active site, in correlation with the oxidation state of the sulfur atom [28].

In this work, we investigated the antitumor activity of the selective COX-2 inhibitors **VA1213**, **VA692**, and **VA694** in cellular models of colorectal cancer and triple-negative breast cancer, and their activity was compared to that of celecoxib.

2. Materials and methods

2.1 Molecules.

Compounds **VA1213**, **VA692**, **VA694** and celecoxib (Figure 1) were synthesized according to previously reported procedures [28]. All compounds were solubilized in Dimethyl Sulfoxide (DMSO, Merck KGaA Darmstadt, Germany). Stock solutions at a concentration of 100 mM were prepared in DMSO and stored at -20 °C until used for experiments. Compounds were subsequently diluted in Dulbecco's Modified Eagle Medium (DMEM) with Fetal Bovine Serum (FBS), according to the experimental model, at the concentrations specified by the protocol, and kept on ice until cellular stimulation. Recombinant human Epidermal Growth Factor (EGF) was supplied by PeproTech (Rocky Hill, NJ, USA).

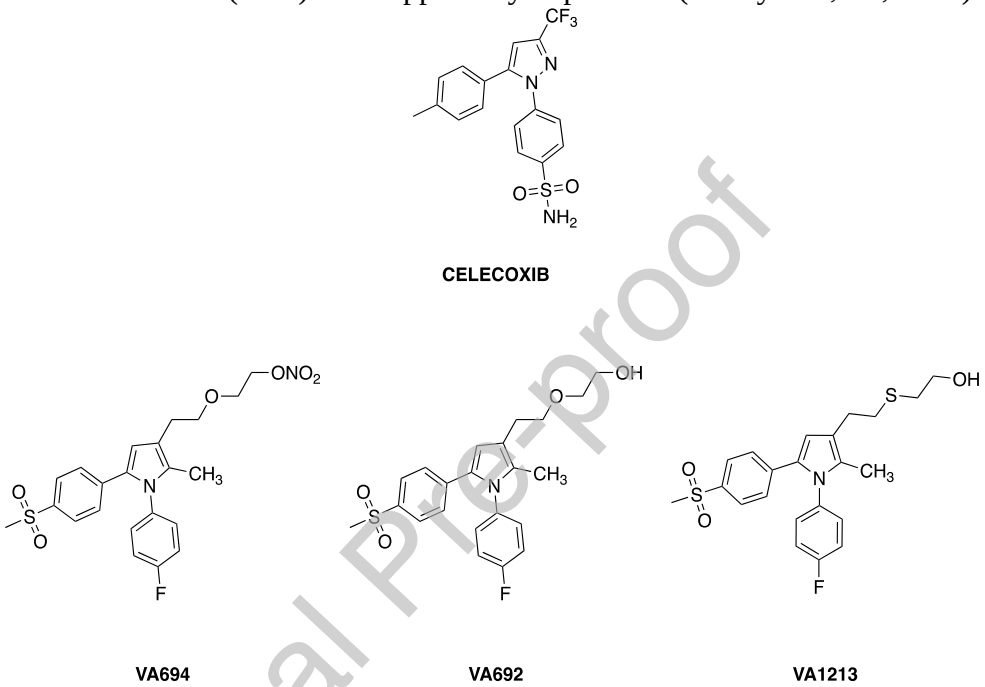

Figure 1: Chemical structure of COX-2 inhibitors

2.2 Cell lines and culture conditions.

The human colorectal carcinoma cells HT-29 and HCT-116, triple-negative breast cancer cells MDA-MB-231 and MCF-7 were purchased from American Type Culture Collection (Manassas, VA, USA). Cells were cultured in DMEM 4500 high glucose (Euroclone SpA, Milan, Italy) supplemented with 10 % FBS (Euroclone SpA, Milan, Italy), 2 mM glutamine, 100 units/mL penicillin and 0.1 mg/mL streptomycin (Merck KGaA, Darmstadt, Germany). Tumor cells were cultured in 10 cm diameter Petri dishes maintained in a humidified atmosphere with 5 % CO_2 and split 1:6 twice a week. All tumor cells were expanded and used until passage 20.

2.3 MTT viability assay.

Cell viability was evaluated using the MTT assay (3-(4,5-dimethylthiazol-2-yl)-2,5-diphenyl tetrazolium bromide, Merck KGaA, Darmstadt, Germany) [29]. Tumor cells (3×10^3) were seeded into 96-well plates containing medium supplemented with 10 % FBS. The following day, the cells were treated with logarithmically increasing concentrations (0-300 µM) of **VA1213**, **VA692**, **VA694**, and celecoxib, and incubated for 24, 48, and 72 h in medium with 10 % FBS at 37 °C. After each incubation period, the medium was replaced with MTT solution (0.5 mg/mL), and the cells were further incubated for 4 h at 37 °C. Formazan crystals were subsequently dissolved in DMSO (Merck KGaA, Darmstadt, Germany), and

absorbance was measured at 540 nm using a multiplate reader (F200 Pro, Tecan Life Sciences, Switzerland).
Cell viability data were expressed as percentage of residual survival, normalizing untreated control cells to 100%. Data analysis was carried out using GraphPad Prism version 8 (GraphPad Software, San Diego, CA, USA). IC_{50} values for each compound at 24, 48, and 72 h were determined by non-linear regression analysis (log[inhibitor] vs. response – variable slope [four parameters]) using the same software.

2.4 Cell cycle assessment.
Cell cycle distribution was analyzed using flow cytometry after propidium iodide staining. Colon cancer cells (7×10^5) were seeded in 6-multiwell plates in growth medium with 10% FBS for 24 h and left to attach overnight. After starving in medium with 0.1 % FBS for 24 h, cells were treated with **VA1213** and celecoxib (20 µM) for 24 h. Cells were then washed three times with PBS, trypsinized, and collected by centrifugation at 0.3 × g for 5 min. The cells were fixed overnight in 80 % ethanol at -20 °C, then washed twice with PBS and incubated with 0.5 mL of PBS containing 100 µg/mL RNase (Thermo Fisher Scientific, Inc. Waltham, Massachusetts, USA) and 50 µg/mL propidium iodide (Merck KGaA Darmstadt, Germany) at 37 °C for 30 min. Cell cycle distribution was analyzed by measuring DNA content using a flow cytometer (BD Biosciences, Milan, Italy). Data were analyzed in triplicate by Cell Quest Pro (BD Biosciences, Milan, Italy) [30].

2.5 Clonogenic assay.
For the clonogenic assay, HT-29 cells were seeded into 6-well plates at a density of 100 cells per well in a medium containing 10 % FBS. The plates were then incubated at 37 °C with 5 % CO_2 in a humidified environment for 24 h to allow cell adhesion. Cells were treated with **VA1213** and celecoxib (20 µM) every 48 h and maintained under incubation for one week. Colonies were fixed using a rapid-staining fixative (Panoptic No.1) for 15 minutes at room temperature, followed by staining with eosin (Panoptic No.2) for 15 minutes. A final staining step was performed using a blue dye (Panoptic No.3; Azur B-based; PanReac AppliChem ITW Reagents, Darmstadt, Germany) for 15 minutes at room temperature.
Images of the colonies were captured using a contrast microscope (Nikon Eclipse TE 300, Nikon, Tokyo, Japan). The results are presented as the fold change in the number of colonies (containing more than 50 cells) relative to the control (untreated cells), which was arbitrarily assigned a value of 1.

2.6 Migration assay.
The scratch assay was used to assess adherent HT-29 cell migration upon COX-2 inhibitors treatments (**VA1213** and celecoxib). HT-29 cells were seeded 6×10^5 cells per well (24-well plate). After having reached the confluence, cells were wounded by scratching with a sterile pipette tip and subsequently washed with PBS to eliminate impaired cells. The medium was changed to a fresh medium with 10 % FBS. The cells were subjected to **VA1213** and celecoxib treatment for 18 h. The wound area was measured using Image-J software (NIH, Bethesda, MD, USA). Images of the wound in each well were acquired from 0 to 18 h under a phase contrast microscope (Nikon Eclipse TE 300, Nikon, Tokyo, Japan). The rate of migration was measured by quantifying the uncovered area of the wound, which cells covered starting from the edge of the scratch, using Fiji software (2.16.0). The results are expressed as the percentage of the wound area covered [31].

2.7 Prostaglandin E2 Express ELISA Assay.

Tumor cells (HT-29 and MDA-MB-231) at the density of 3×10^4/well were plated into 24-well plates. After adherence medium was changed with 1% FBS medium and cells were incubated for 24 h with COX-2 inhibitors (20 μM). To replenish COX-2 substrate pool, arachidonic acid (10 μM, Merck KGaA Darmstadt, Germany) was added to the cells. Conditioned media were collected and PGE2 levels were measured using an EIA kit (Prostaglandin E2 Express ELISA kit-Monoclonal, Cayman Chemical, Ann Arbor, MI USA). Data are reported as pg/mL. As a reference, cells were fixed, stained, and counted.

2.8 Cyclooxygenase (COX) activity assay

COX-1 and COX-2 activity was evaluated using the manufacturer's protocol (ab204699, Abcam, Cambridge, UK). The assay quantifies COX peroxidase activity by measuring the conversion of arachidonic acid into prostaglandin G2 (PGG2), which reacts with a fluorescent probe to generate a signal proportional to enzyme activity.

PGG2 production was then examined in two complementary experimental setups to assess the COX-2 selectivity of **VA1213** and celecoxib. In the first setup, COX activity was measured in HT-29 protein lysates treated with **VA1213** or celecoxib either alone or after pre-incubation with the COX-1–selective inhibitor SC-560. This allowed us to determine whether PGG2 reduction remained consistent when COX-1 was blocked. In the second setup, PGG2 formation was measured using purified COX-1 enzyme to directly compare the inhibitory effects of **VA1213** and celecoxib on COX-1. Together, these analyses provided complementary evidence for the relative COX-1/COX-2 selectivity of VA1213.

Briefly, 6×10^6 HT-29 cells were scraped in Lysis buffer, subjected to two freeze–thaw cycles, and centrifuged at 200 × g for 5 minutes. The supernatant was then collected and quantified. For each reaction, 180 μg of protein (20 μL of sample) were mixed with 68 μL of reaction mix and 2 μL of either a COX-specific inhibitor (SC560, celecoxib, or **VA1213**) or DMSO as vehicle in a 96-well plate. Each condition was tested in duplicate wells. The reaction was initiated by adding arachidonic acid solution, following the manufacturer's protocol. Fluorescence was subsequently measured (Ex/Em = 535/587 nm) in kinetic mode every 3 minutes for 30 minutes (Synergy HTX multi-mode reader, BioTek, Winooski, VT, USA)

2.9 Western blot.

Western blot was performed on cell lysates. Tumor cells (3×10^5/dish) were seeded in 60 mm Petri plates. After adherence, cells were starved for 18 h and then treated with **VA1213**, **VA692**, **VA694**, or celecoxib (20 μM) for 24 h in medium containing 10 % FBS. In a second experimental protocol, cells were starved for 18 h and subsequently treated with **VA1213** (10 and 20 μM) for 24 h and with PGE2 (1 μM for 15 minutes) where appropriate. In the final protocol, tumor cells were starved for 18 h, then preincubated with **VA1213** (20 μM), and subsequently exposed to EGF (25 ng/ml) for 3 min.

At the end, cells were washed 2 times with cold Dulbecco's Phosphate Buffered Saline (PBS) (Merck KGaA Darmstadt, Germany) and lysed on ice with RIPA Lysis Buffer 10X, supplemented with 2 mM Na_3VO_4 and 1x Protease inhibitor cocktail for mammalian cells (Merck KGaA Darmstadt, Germany) as described previously [29]. Cell lysates (derived from cell cultures) were centrifuged at maximum speed for 20 minutes at 4 °C and the supernatants were then collected. Bradford assay was used to determine the protein concentration. Proteins (50 μg/sample) were separated by polyacrylamide gel electrophoresis (Bolt 4 to 12 %, Bis-Tris, 1.0 mm, Mini Protein Gel, 10-well, from Thermo Fisher Scientific, Inc.). Proteins were transferred onto a nitrocellulose membrane (iBlot 2 Transfer Stacks, nitrocellulose, regular size from Thermo Fisher Scientific, Inc.). Next, membranes were blocked with 5 % non-fat dried milk for 1 h at room temperature, and then incubated at 4 °C overnight with primary

antibody including anti-COX-2 (mouse, 1:1000) provided by Cayman Chemical, Ann Arbor, MI USA), CDK2 (rabbit, 1:1000), CDK4 (rabbit, 1:1000), Cyclin D1 (rabbit, 1:1000), Cyclin D3 (rabbit, 1:1000), p21 (rabbit, 1:1000), caspase 3 (rabbit, 1:1000), cleaved caspase-3 (Asp175) (rabbit, 1:1000), pERK1/2 (rabbit 1:2000), ERK1/2 (rabbit, 1:1000), pAKT (ser473) (rabbit 1:1000), anti-AKT (mouse 1:2000), pEGFR (rabbit, 1:1000) and EGFR (rabbit, 1:1000) purchased from Cell Signaling Technology (Danvers, MA, USA). Anti-β-actin antibody (mouse, 1:10,000) was from Merck KGaA (Darmstadt, Germany).
The membranes were washed three times (with PBS and TWEEN20 0.5 %) and then incubated with secondary antibodies, HRP conjugated (anti-rabbit, 1:2500, cat. n. W401B; anti-mouse 1:2500, cat. n. W402B, both from Promega Corporation Madison, Wisconsin, USA) at room temperature for 1 h. At the end of incubation, membranes were washed with PBS and TWEEN20 0.5 % (Merck KGaA. (Darmstadt, Germany) three times. The analysis of protein bands was conducted using ChemiDoc XRS (Bio-Rad Laboratories, Inc. Milan, Italy) after incubating the membranes at room temperature for 2 minutes with an enhanced chemiluminescent substrate (Bio-Rad Laboratories, Inc. Milan, Italy) [32].

2.10 Statistical analysis.

Results are expressed as means ± SD or ± SEM. Statistical analysis was carried out using Student's t test, two-way ANOVA, followed by Bonferroni post-test for multiple comparisons as appropriate. $P<0.05$ was considered statistically significant. Data was analyzed and graphed using GraphPad Prism 8 (GraphPad Software, MA, USA).

3. Results

3.1 Antiproliferative effect of COX-2 inhibitors on tumor cell lines.

To investigate the pharmacological activity of COX-2 inhibitors on interfering with tumor cell proliferation, MTT survival test was performed. HT-29, and MDA-MB-231 cells were treated for 24, 48, and 72 h with increasing logarithmically concentrations (1-300 μM) of **VA1213**, **VA692**, **VA694**, and celecoxib. Celecoxib was selected as a commercial control to be compared with the compounds under investigation.

In HT-29 cells, under growth-promoting conditions (medium supplemented with 10% FBS), celecoxib exhibited the greatest potency among all COX-2 inhibitors after 24 h, with an IC_{50} of 39.26 ± 2.93 μM. **VA1213** and **VA694** showed IC_{50} values of 66.28 ± 3.44 μM and 71.35 ± 5.42 μM, respectively (Figure 2A and Table 1). **VA692** was less effective at inhibiting the viability of HT-29 cells at 24 h, with an IC_{50} exceeding 100 μM (Table 1). However, a concentration of 300 μM was found to be toxic for all tested compounds (Figure 2A).

After 48 h of treatment, compound **VA1213** emerged as the most potent among the compounds under investigation, displaying comparable efficacy to celecoxib (Figure 2C). The IC_{50} value for **VA1213** at 48 h was 26.68 ± 3.02 μM, while that for celecoxib was 31.16 ± 2.64 μM (Table 1). At this time point, **VA692** remained the least active compound, with an IC_{50} of 79.59 ± 6.15 μM, whereas **VA694** exhibited intermediate activity (IC_{50}: 51.52 ± 4.43 μM).

VA1213 maintained superior potency among the COX-2 inhibitors even after 72 h of exposure, as confirmed by IC_{50} values (Figure 2E and Table 1). It exhibited a distinct pharmacodynamic profile characterized by a time-dependent increase in potency: its IC_{50} decreased from 66.28 ± 6.44 μM at 24 h to 26.68 ± 3.02 μM at 48 h, remaining stable up to 72 h (IC_{50}: 28.01 ± 2.33 μM) (Table 1, Figure 2E). The potency of **VA1213** at longer time points (48 and 72 h) was comparable to that of celecoxib, which, by contrast, exhibited a rapid cytotoxic effect within the first 24 h that remained stable through 72 h. A weak antiproliferative effect was observed for compound **VA692** at equimolar concentrations compared to the other tested compounds on HT-29 cells, whereas **VA694** exhibited intermediate activity, falling between the more potent compounds (**VA1213** and celecoxib) and the less active **VA692** (Figure 2A, C, E).

In MDA-MB-231 cells, the compounds exhibited weak concentration-dependent antiproliferative activity after 24 h of exposure (Figure 2B). **VA1213** showed a lower ability to inhibit cell survival compared to its effect in HT-29 cells. Among the tested compounds, **VA692** was the least active, whereas celecoxib demonstrated the highest potency, with an IC_{50} value comparable to that observed at 24 h in HT-29 cells (44.24 ± 6.42 μM).

After 48 h of treatment, celecoxib exhibited a strong cytotoxic effect, with an IC_{50} of 29.99 ± 3.77 μM, whereas **VA1213** showed an IC_{50} of 62.81 ± 4.88 μM. For **VA694**, the IC_{50} exceeded 100 μM, while for **VA692** it reached approximately 150 μM (Figure 2D and Table 1). Interestingly, at 72 h, **VA1213** was equipotent to celecoxib, while **VA694** exhibited an intermediate IC_{50} value, and **VA692** remained the least active compound (Figure 2F and Table 1).

To clarify the contribution of COX-2 expression from tumor-type–specific factors, two additional cancer models, MCF-7 and HCT-116, expressing moderate and low COX-2 levels, respectively (Figure 2G and H), were included, enabling evaluation of whether compound activity was driven by target abundance rather than by the cellular background.

HCT-116 cells were less sensitive, showing IC_{50} values of 148.9 ± 19.81 μM at 24 h (Figure 2I), 86.90 ± 9.03 μM at 48 h (Figure 2K) and 72.73 ± 8.07 μM at 72 h (Figure 2M). In contrast, MCF-7 cells displayed a clearer time-dependent cytotoxic response, with IC50 values decreasing from 71.81 ± 8.12 μM at 24 h (Figure 2J) to 51.74 ± 4.42 μM at 48 h

(Figure 2L) and 43.32 ± 2.18 µM at 72 h (Figure 2N), although the potency did not reach that observed in HT-29 cells (Table 2). Celecoxib treatment affected both cell lines, and the difference in sensitivity between MCF-7 and HCT-116 was less marked (Table 2). In conclusion, HT-29 and MCF-7 cells exhibited a greater antiproliferative response to the compounds under investigation than MDA-MB-231 and HCT-116 cells. Among the compounds tested, **VA1213** showed the highest potency, comparable to celecoxib. Sub-toxic concentrations of 10 and 20 µM were selected to investigate early cellular responses at 24 h, as these doses are non-cytotoxic at this time point but approach the IC_{50} at 48 h, allowing the study of initial molecular events preceding cell death.

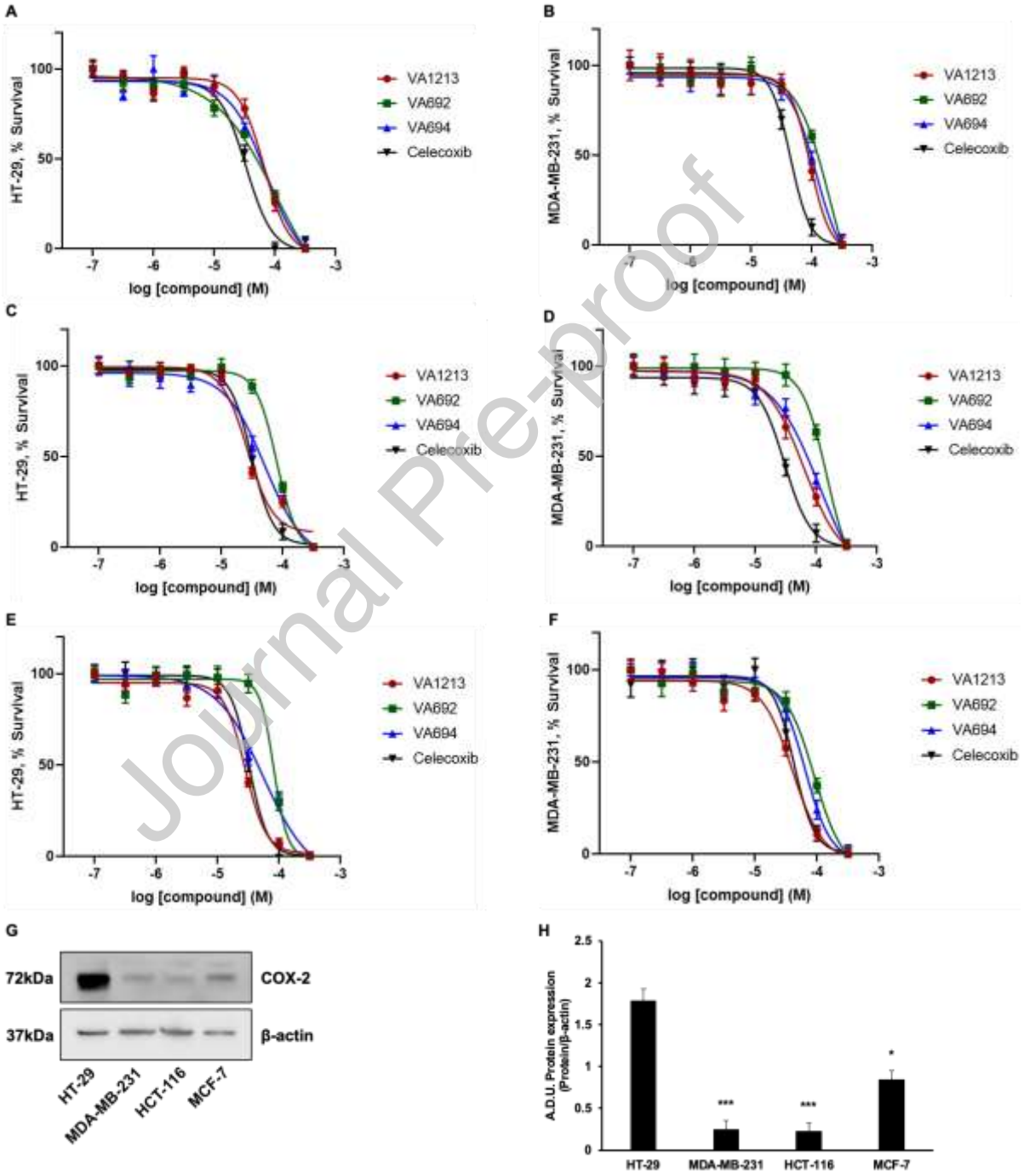

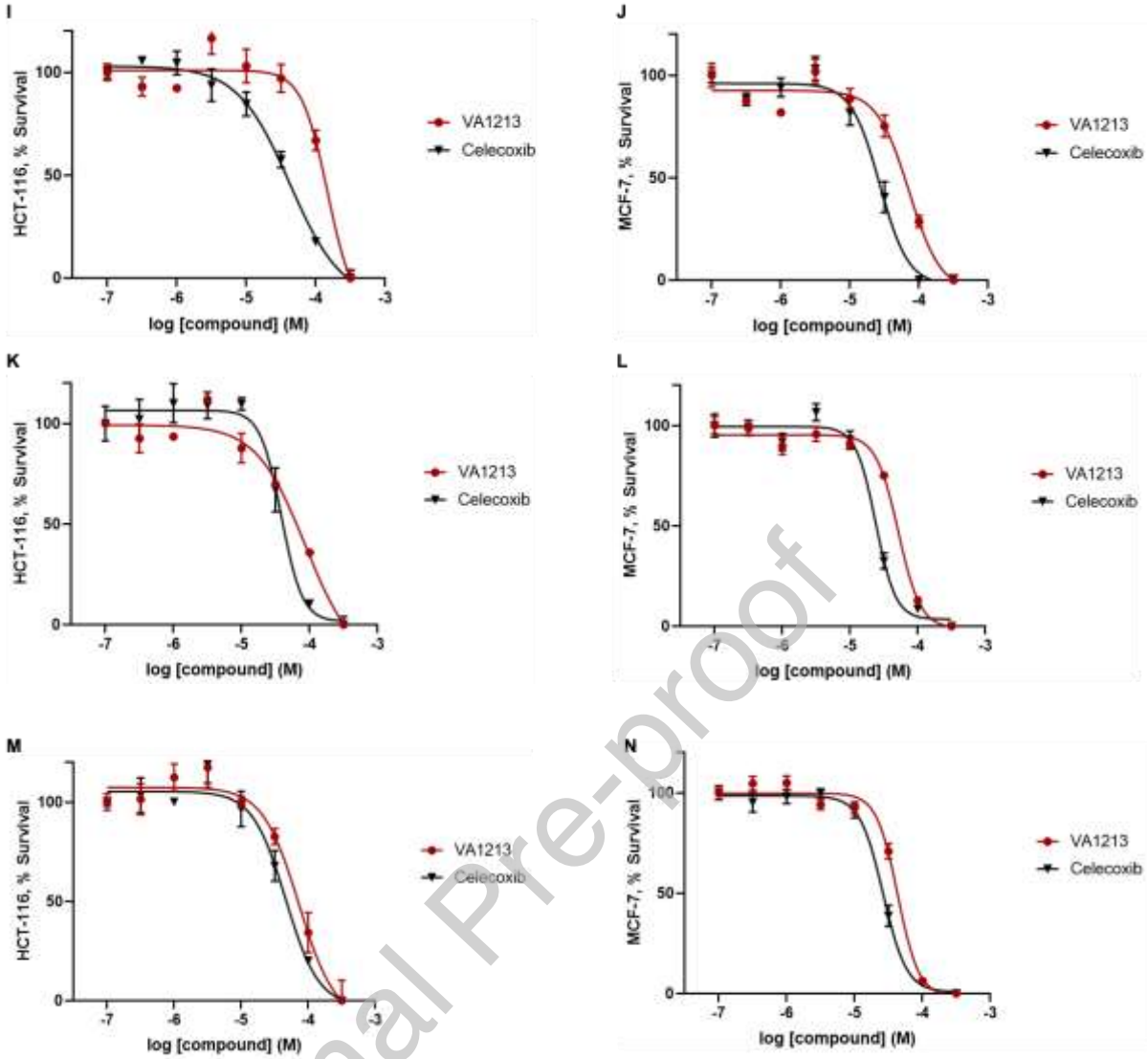

Figure 2. COX-2 inhibitors suppress tumor cells growth. HT-29 (A, C, E) and MDA-MB-231 (B, D, F) were treated with increasing concentrations of COX-2 inhibitors (0.1-300 µM) in medium with 10 % FBS for 24 h (A for HT-29 and B for MDA-MB-231), 48 h (C for HT-29 and D for MDA-MB-231) and 72 h (E for HT-29 and F for MDA-MB-231). (G). COX-2 basal expression in HT-29, MDA-MB-231, HCT-116 and MCF-7 cells. Blot shown is representative of three experiments with similar results. (H). Quantification of blot in (G) reported as Arbitrary Densitometry Units (A.D.U.) ± SD of COX-2 vs β actin which was used as loading control. *$p \leq 0.05$, ***$p \leq 0.001$ vs. HT-29. HCT-116 (I, K, M) and MCF-7 (J, L, N) were treated with increasing concentrations of **VA1213** and celecoxib (0.1-300 µM) in medium with 10 % FBS for 24 h (I for HCT-116 and J for MCF-7), 48 h (K for HCT-116 and L for MCF-7) and 72 h (M for HCT-116 and N for MCF-7). Cell viability was tested by MTT assay. Dose–response curves were generated using GraphPad Prism 8 software, fitting data with a four-parameter logistic (4PL) model. Data are expressed as percentage of cell viability relative to untreated controls, which were set at 100%, and are presented as mean ± SD (n = 3).

Table 1. IC_{50} in HT-29 and MDA-MB-231 cells

	IC_{50} (µM ± SD) on HT-29			IC50 (µM ± SD) on MDA-MB-231		
	24 h	**48 h**	**72 h**	**24 h**	**48 h**	**72 h**
VA1213	66.28±3.44	26.68±3.02	28.01±2.33	93.8±6.94	62.81±4.88	40.28±4.31
VA692	107.7±8.63	79.59±6.15	81.98±6.91	200.6±7.01	141.7±6.69	90.01±7.16
VA694	71.35±5.42	51.52±4.43	55.52±4.34	116.5±6.29	113.7±5.03	64.23±3.55
Celecoxib	39.26±2.93	31.16±2.64	32.47±2.86	44.24±6.42	29.99±3.77	42.95±5.91

Table 2. IC_{50} in HCT-116 and MCF-7

	IC_{50} (µM ± SD) on HCT-116			IC50 (µM ± SD) on MCF-7		
	24 h	**48 h**	**72 h**	**24 h**	**48 h**	**72 h**
VA1213	148.9± 19.81	86.90± 9.03	72.73± 8.07	71.81± 8.12	51.74± 4.42	43.32± 2.18
Celecoxib	42.29± 5.53	38.48± 4.42	46.08± 5.69	27.75± 3.19	24.6± 2.53	26.50± 1.17

IC_{50} values were calculated by the use of GraphPad Prism 8 software on the data of graphs reported in Figure 2A-L.

3.2 Evaluation of COX-2 inhibition and selectivity in tumor cells *in vitro*

To further investigate the different responses of tumor cells to the antiproliferative activity of COX-2 inhibitors, a target validation was performed.

Western blot analysis revealed that COX-2 expression varies between the four cell lines (Figures 2G and H). Specifically, starting from the same protein content, HT-29 cells exhibited high levels of the protein followed by MCF-7, whereas in MDA-MB-231 and HCT-116 cells COX-2 levels were significantly lower.

Accordingly, to evaluate the extent of COX-2 inhibition exerted by the compounds under investigation, the levels of PGE2, one of the principal terminal metabolites of the arachidonic acid cascade, were quantified in HT-29 and MDA-MB-231. PGE2, synthesized via microsomal prostaglandin E synthase-1 (mPGES-1) downstream to COX-2, is a critical pro-tumorigenic mediator implicated in the pathogenesis and progression of both colorectal and breast cancer [33]. Using an ELISA assay, PGE2 was quantified in cell-conditioned media, and a significant increase in its production was observed in the presence of arachidonic acid, a precursor added to replenish intracellular substrate stores. After 24 h of treatment with the compounds under investigation, tested at a concentration of 20 μM, a marked reduction in the production of soluble prostaglandin in the medium was recorded. In line with the protein analysis, HT-29 cells showed a production and release capacity of around 700 pg/mL (Figure 3A), whereas MDA-MB-231 cells, which express lower levels of COX-2, produced less than 100 pg/mL of PGE2 within 24 h (Figure 3B).

Next, we examined the selectivity of the compounds toward human COX in HT-29 lysates using a time-course assay monitoring PGG2 production. Based on previous evidence identifying **VA1213** as the most COX-2–selective compound [28], we evaluated its activity toward both COX-1 and COX-2 in this system, including celecoxib as a reference inhibitor. Both compounds were tested at 100 nM, consistent with reported Ki values of 8 nM and 61 nM for **VA1213** and celecoxib, respectively [28]. COX-1/2 activity was followed over a 30-minute incubation (time-course profiles in Supplementary Figure 1A–1C), and PGG2 formation was quantified by calculating the area under the curve (AUC; Figure 3C–3D).

In HT-29 lysates, the COX-1–selective inhibitor SC560 caused only a modest AUC reduction (~15%), indicating that COX-1 contributes minimally to PGG2 production in this context. In contrast, **VA1213** and celecoxib decreased the AUC by approximately 50% and 60%, respectively (Figure 3C and Supplementary Figure 1A–1B). SC560 pretreatment did not further lower PGG2 levels when combined with **VA1213** or celecoxib, as AUC values were comparable to those obtained with each inhibitor alone. These results indicate that the inhibitory effects of **VA1213** and celecoxib primarily reflect COX-2 targeting.

Consistently, the isolated COX-1 assay confirmed complete suppression of PGG2 generation by SC560, while **VA1213** showed no measurable effect and celecoxib induced only minimal inhibition (Figure 3A and Supplementary Figure 1C). Overall, these findings strongly suggest that **VA1213** maintains a clear COX-2–selective profile in HT-29 cells, closely matching the inhibitory pattern observed for celecoxib.

Overall, all tested compounds, **VA1213**, **VA692**, **VA694**, and celecoxib, markedly reduced PGE2 production to near baseline in both cell lines. In terms of selectivity, **VA1213** displayed clear COX-2 preference. Based on their higher sensitivity and responsiveness, HT-29 cells were chosen for subsequent molecular experiments.

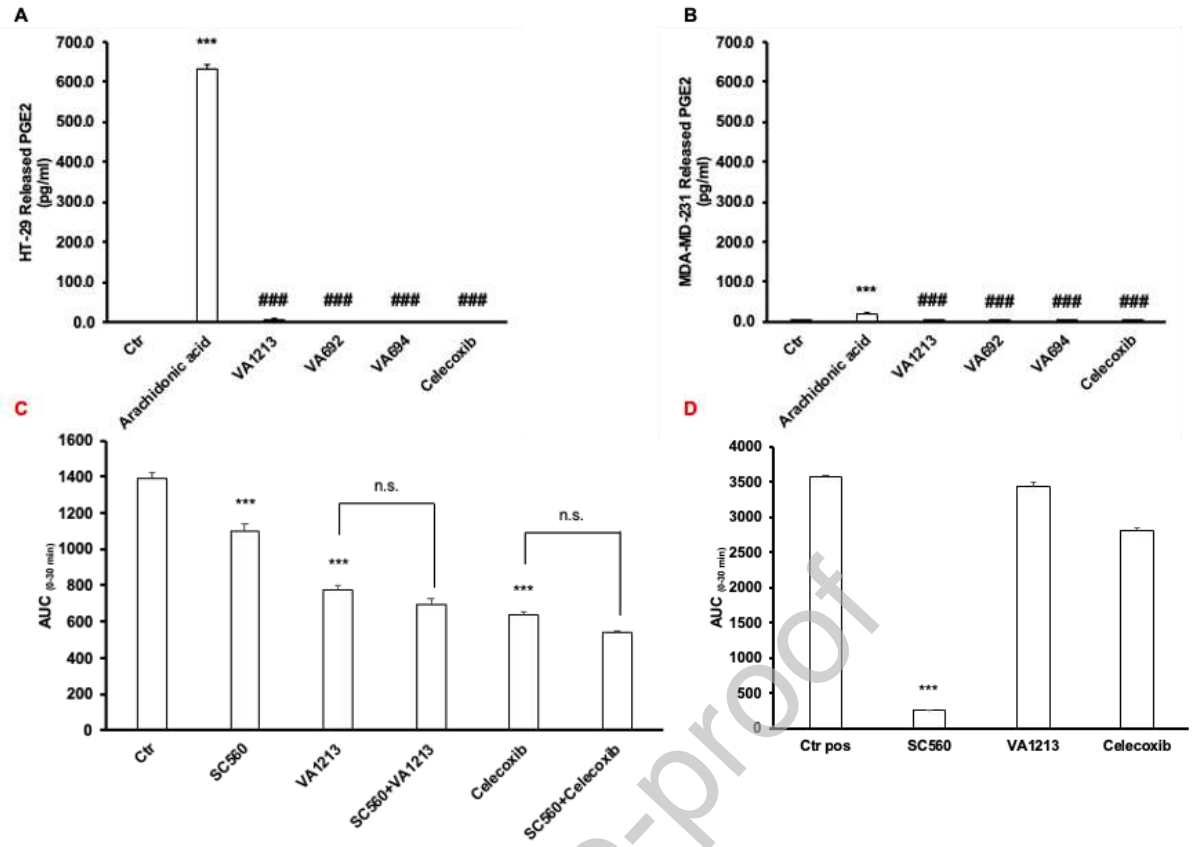

Figure 3. Evaluation of COX-2 inhibition and selectivity in tumor cells. ELISA assay for PGE2 measurement in the supernatant of HT-29 (A) and MDA- MB-231 (B) treated with **VA1213**, **VA692**, **VA694**, and celecoxib (20 μM) after 24 h in the presence of arachidonic acid (10 μM). ***p ≤ 0.001 vs Ctr (untreated cells). ###p≤ 0.001 vs Arachidonic acid alone. (C). Time-course of PGG2 formation in HT-29 cell lysates and (D) isolated human COX-1 following treatment with SC560, VA1213 (100 nM), celecoxib (100 nM), or their combinations, reported as area under the curve ($AUC_{0–30}$ min).Data are reported as mean ± SD. ***p ≤ 0.001 vs Ctr or Ctr pos (untreated cells) (ANOVA test).

3.3 VA1213 regulates cell cycle checkpoint proteins and apoptosis in colorectal cancer cells

Cell cycle arrest and apoptosis constitute the two major cellular events leading to the impaired proliferation of cancer cells due to anticancer agents [34].

To investigate whether cell cycle arrest contributes to the inhibition of HT-29 cell growth, cell cycle regulatory proteins were analyzed following treatment with a sub-cytotoxic dose (20 μM) to capture early molecular changes prior to any loss of viability measured at 24 h.

Analysis of cell cycle regulators, including CDKs and CDK inhibitors (CDKis), revealed that **VA1213**, and to a lesser extent celecoxib, induced a significant increase in the expression of the tumor suppressor protein p21 (Figures 4A and 4B), which is a cyclin-dependent kinase inhibitor, known to be involved in arresting the cell cycle at the G1, G2, or S phase. Interestingly, **VA1213** significantly reduced the expression of cyclin D1, D3, CDK2, and CDK4, which are key regulators mediating the transition from G1 to S phase. Celecoxib exhibited a statistically significant reduction in cyclin D3 expression. At the same concentration, **VA692** and **VA694** did not exhibit activity on the analyzed cell cycle regulatory proteins (Figures 4A and 4B).

Building on the observed regulation of cyclins and CDKs, mainly affected by **VA1213**, we investigated cell cycle progression through flow cytometry. Results showed that the treatment with **VA1213** (20 µM) caused a significant increase in the apoptotic cells represented by sub G0/G1 population which was accompanied by a reduction of the number of cells in the G2/M phase (Figure 4C). At the same concentration, celecoxib was not effective in altering the distribution of cells across the different phases of the cell cycle (Figure 4C).

Based on our data indicating that **VA1213** induced G0/G1 phase cell cycle arrest by modulating cyclin D1, D3, CDK2, CDK4, and p21, as well as promoting the induction of a sub-G0/G1 peak, a hallmark of apoptosis, we aimed to assess the cleavage of the apoptotic effector caspase-3 after 24 h of exposure. **VA1213** induced a concentration-dependent cleavage of caspase-3, the final effector of the apoptosis cascade (Figures 4D and 4E), clearly demonstrating that colon cancer cell death occurs in a caspase-3-dependent manner.

To determine whether the time-dependent cytotoxicity of **VA1213** relative to celecoxib observed in Figure 2 was associated with slower cumulative alterations in cell-cycle progression and pro-apoptotic signaling, we examined the expression of p21 and cleaved caspase-3 at early time points (6 and 12 h) following treatment with either **VA1213** or celecoxib. As shown by our results, celecoxib induced a marked upregulation of p21 as early as 6 h, whereas **VA1213** produced a slower and more gradual increase in p21 expression (Supplementary Figure 2A and B).

In contrast, caspase-3 cleavage was minimal at 6 h for both treatments but showed marked activation by 12 h for both treatments (Supplementary Figure 2C and D). It is plausible that celecoxib also acts through caspase-3–independent mechanisms capable of inducing p21 upregulation as early as 6 h. At 12 h, caspase-3 activation becomes significantly increased for both compounds, consistent with the toxicity data measured at 24 h.

These data demonstrated that sub-toxic concentrations (20 µM) of **VA1213** induce cell cycle arrest through the regulation of checkpoint proteins involved in the cell cycle, p21 induction, accumulation of cells in the G0/G1 phase, and activation of apoptosis via caspase-3 cleavage.

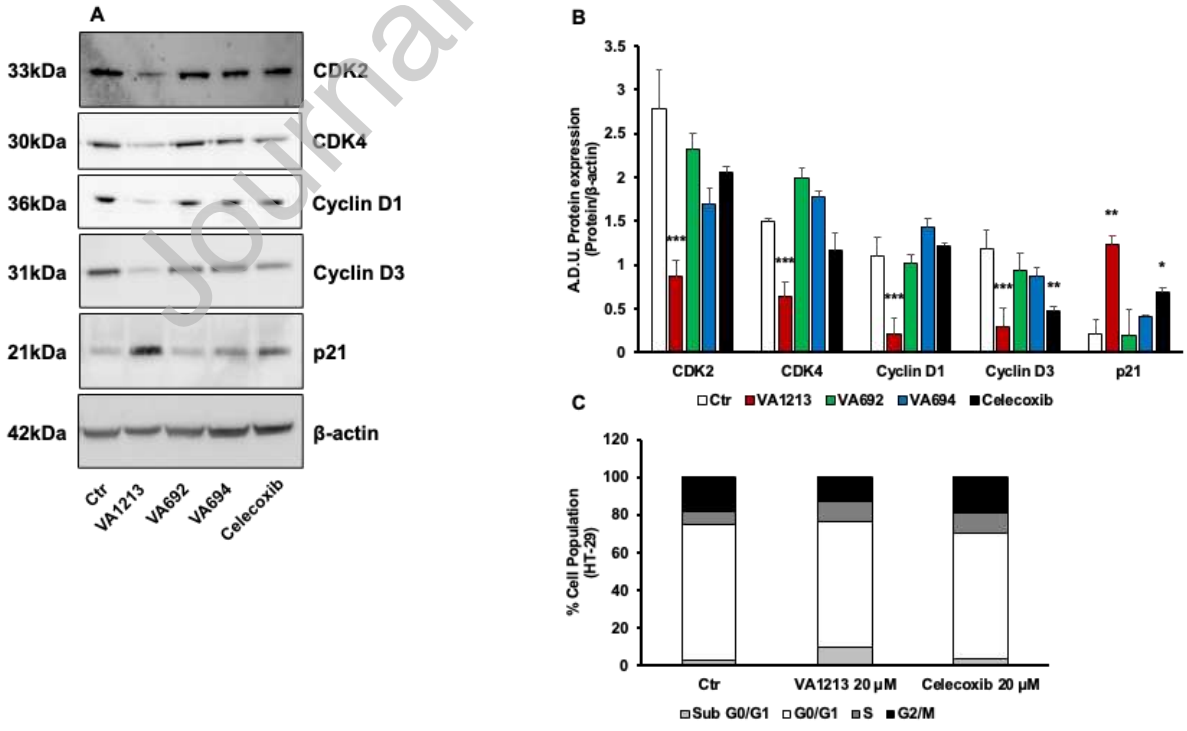

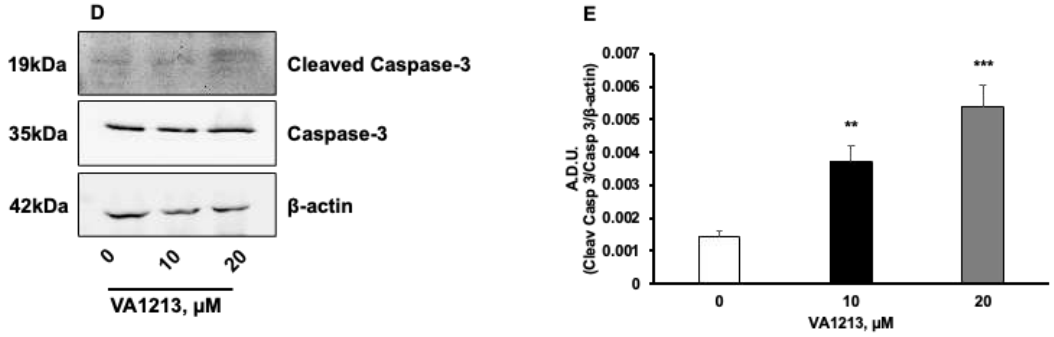

Figure 4. COX-2 inhibitors modulate the cell cycle checkpoint proteins and induces apoptosis in HT-29. HT-29 were exposed to COX-2 inhibitors (20 μM) for 24 h and the cell cycle checkpoint proteins were assessed by western blot (A). (B). Quantification of cell cycle checkpoint proteins in HT-29 reported as Arbitrary Densitometry Units (A.D.U.) ± SD vs β-actin which was used as loading control. *p≤0.05, **p≤0.01 and **p≤0.001 vs. ctr (untreated cells). (C). The percentage of cells at each stage of the cell cycle was analyzed by flow cytometry after DNA staining with propidium iodide. (D). HT-29 cells were exposed to **VA1213** for 24 h and cleaved-caspase 3 was assessed by western blot. (E). Quantification of blot in D. Arbitrary Densitometry Units (A.D.U.) ± SD were reported as Cleaved-Caspase 3/Caspase 3 vs β-actin (n= 3). **p ≤ 0.01 and ***p ≤ 0.001 vs. ctr (untreated cells).

3.4 VA1213 impairs tumor cell migration and colony forming ability

Several studies suggest that COX-2 may significantly promote development and progression of colorectal cancer including metastasis [35]. Cell migration is a measure of the metastatic potential of cancer cells; therefore, the influence of COX-2 inhibitors on cell migration was investigated by the scratch assay [36]. At the same concentration (20 μM), COX-2 inhibition by **VA1213** resulted in a significantly greater reduction in HT-29 migration compared to celecoxib (Figure 5A and B).

Focusing on another property that could also be beneficial in the treatment of malignancies, we investigated the clonogenic capacity of HT-29 cells exposed to COX-2 inhibitors. Both **VA1213** and celecoxib, at a concentration of 20 μM, were effective in significantly reducing the ability to form colonies (Figure 5C and D).

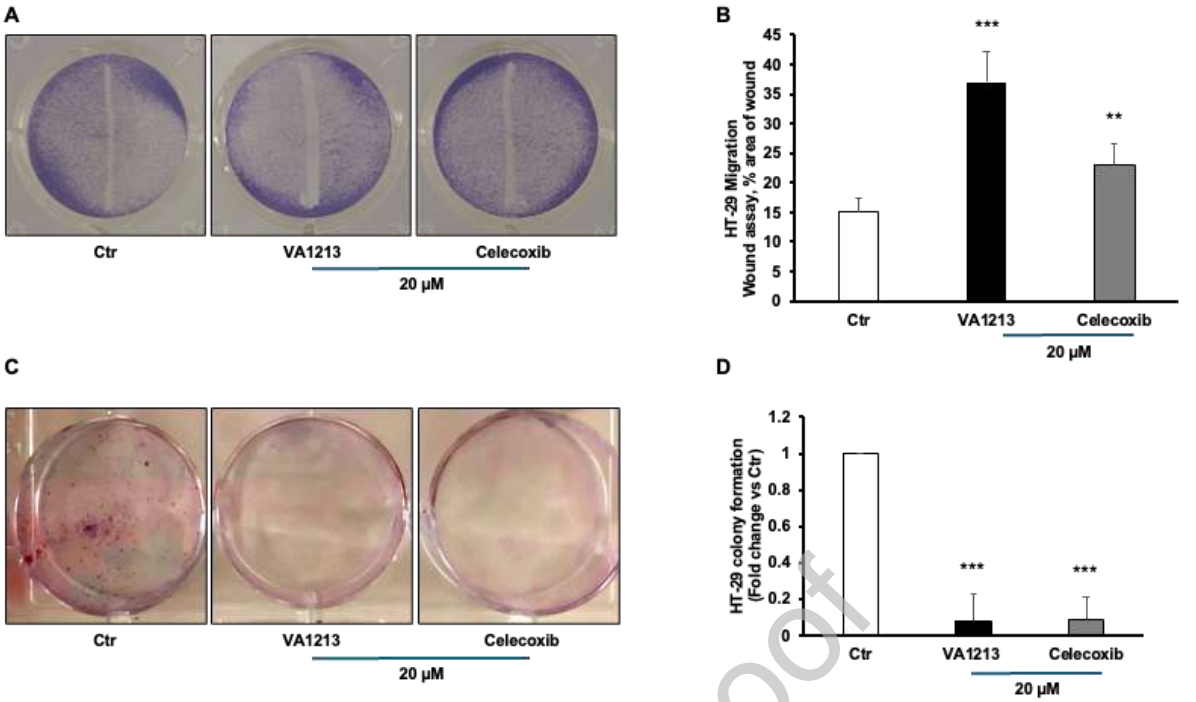

Figure 5. VA1213 inhibits the migration and clonogenicity of HT-29 cells. (A) HT-29 cells were seeded onto 24-well culture plates and grown to confluence in medium containing 10% FBS. The cells were scratched with a sterile tip and subsequently treated with **VA1213** and celecoxib (20 µM) for 18 h. The images are representative of three independent experiments. (B) Quantification of migration. Data are reported as the percentage of migration area ratio (% of area at 18 h/area at 0 h). *p≤0.05 and **p≤0.01 vs. Ctr (untreated cells).
(C). Representative images of clonogenic assay in HT-29 treated with **VA1213** or celecoxib (20 µM) every 48 h. After 7 days, cells were fixed, stained, and photographed. ((D). Quantification of colony number (C) of HT-29 treated with **VA1213** or celecoxib (20 µM) for 7 days. ***p≤0.001 vs. Ctr (untreated cells).

3.5 VA1213 impairs tumor cell response by inhibiting the MAPK, PI3K/AKT pathways and EGFR activation

Aberrant COX-2 signaling is responsible for the activation of the MAPK and PI3K/AKT pathways, leading to cell proliferation and tumor progression [3,37]. Here, we investigated whether **VA1213** could interfere with these signaling pathways. As shown in Figure 6, **VA1213** at 20 µM induced a significant reduction in ERK1/2 (Figure 6A and 6B) and AKT phosphorylation (Figure 6C and 6D), consistent with the proliferation arrest and cell apoptosis seen above.
As EGFR and its activated downstream signaling pathways play a crucial role in colon cancer development and progression, we assessed whether **VA1213** affected receptor activity. Notably, treatment of HT-29 cells with **VA1213** reduced EGFR activation, as indicated by decreased phosphorylation at tyrosine 845 (Figure 6E and 6F).
To assess the role of PGE2, one of the major downstream products of COX-2 activity implicated in tumor progression [4,5], in the activation of EGFR, a rescue experiment was performed using exogenous PGE2. HT-29 cells were treated with 20 µM **VA1213** for 24 h, which resulted in reduced EGFR activation. As shown in Figure 6G and 6H, the addition of PGE2 for 15 minutes induced a statistically significant rescue of EGFR activation.

Of note, no phospho-EGFR reduction was observed in MDA-MB-231 cells (Figure 6I and 6J), which express low levels of COX-2 and high levels of EGFR. This suggests that the inhibition of EGFR activation is a consequence of COX-2 inhibition rather than a direct off-target effect of **VA1213** on EGFR.

To evaluate potential off-target effects of **VA1213** on EGFR, receptor activation was assessed following stimulation with its ligand, EGF, in both cell lines. As shown in Figures 6K-L (HT-29) and 6M-N (MDA-MB-231), preincubation with **VA1213** (20 min) did not interfere with EGF-induced EGFR activation, suggesting that **VA1213** does not exert off-target effects on EGFR. These findings indicate that the reduced phosphorylation of EGFR observed upon VA1213 treatment is a consequence of COX-2 enzymatic inhibition and reduced PGE2 levels.

Collectively, these data demonstrate that **VA1213** inhibits COX-2 activity, thereby leading to decreased activation of EGFR, ERK1/2, and AKT.

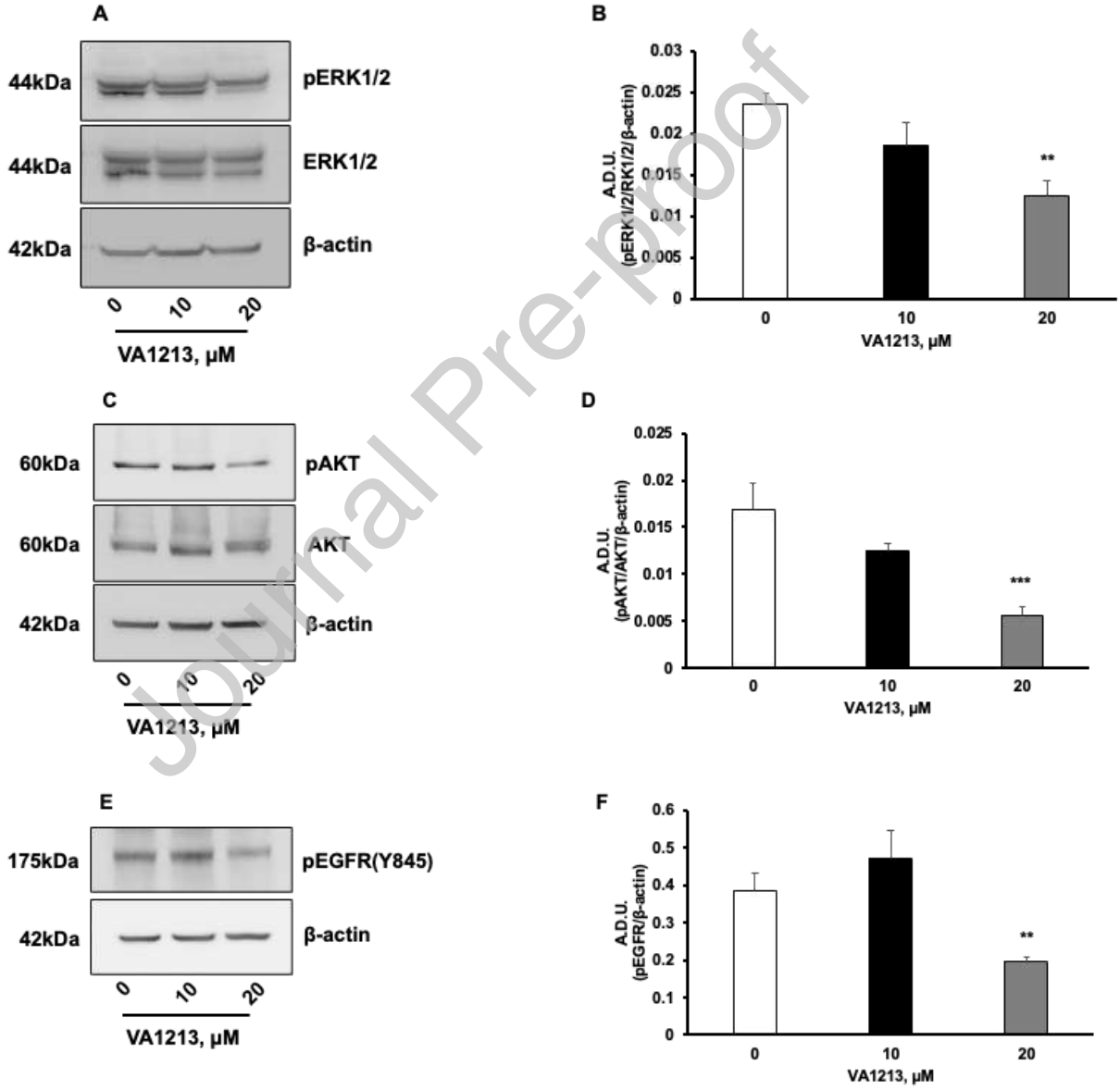

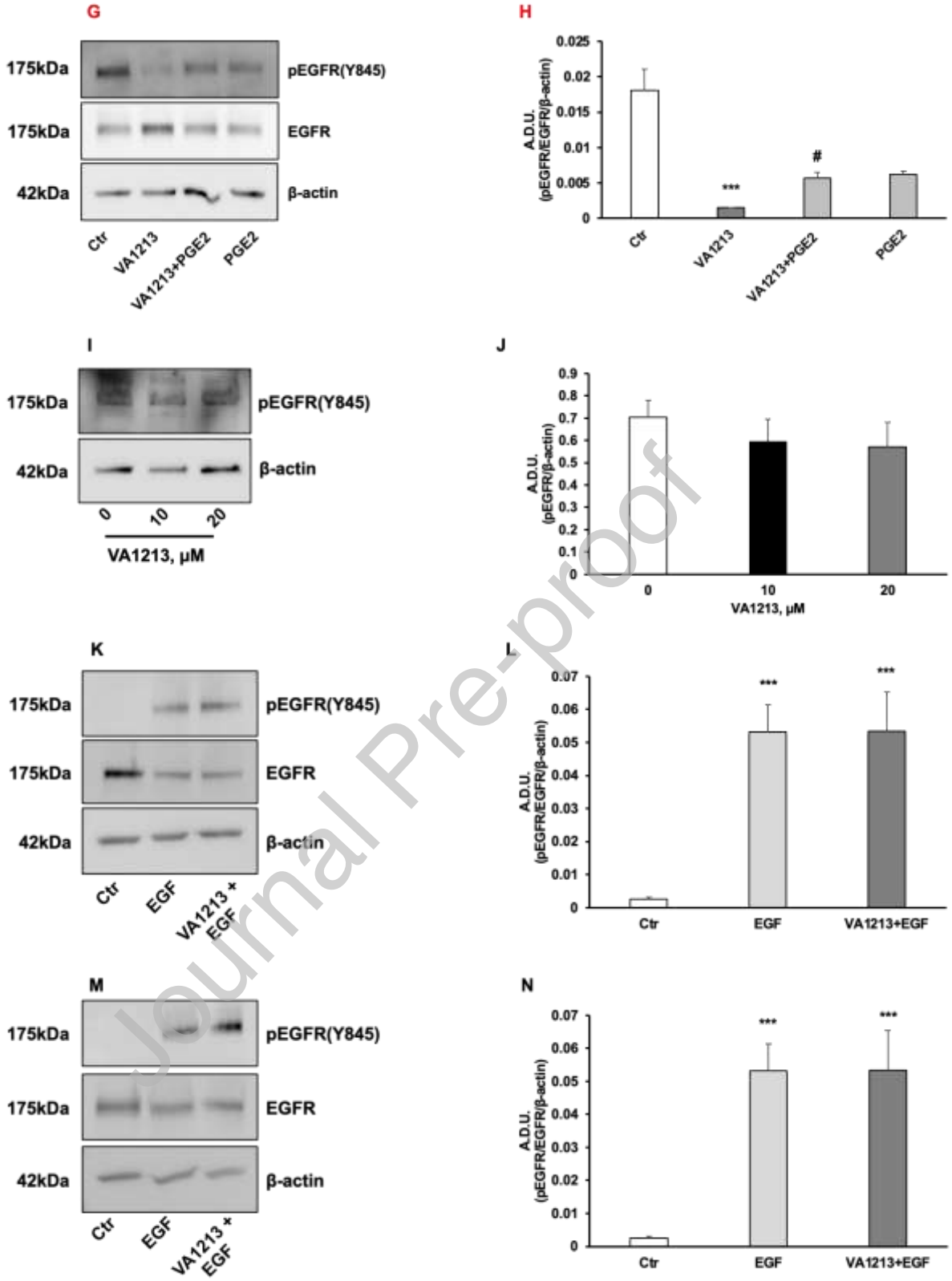

Figure 6. VA1213 exerts antitumor activity by blocking the activation of several signaling cascades. (A). ERK1/2 activation after 24 h of **VA1213** treatment. (B). Quantification of blot in A. Arbitrary Densitometry Units (A.D.U.) ± SD were reported as pERK1/2/ ERK1/2 vs β-actin (n = 3). **p ≤ 0.01 vs. ctr (untreated cells). (C). AKT activation after 24 h of **VA1213** treatment. (D). Quantification of blot in C. Arbitrary Densitometry Units (A.D.U.) ± SD were reported as pAKT/AKT vs β-actin (n =3). ***p ≤0 .001 vs. ctr

(untreated cells). (E). EGFR activation (Y845) after 24 h of **VA1213** treatment in HT-29 cells. (F). Quantification of blot in E. Arbitrary Densitometry Units (A.D.U.) ± SD were reported as pEGFR vs β-actin (n=3). **$p \leq 0.01$ vs. ctr (untreated cells). (G). EGFR activation (Y845) after 24 h of **VA1213** (20 μM) and then exposed to PGE2 (1 μM) for 15 minutes. PGE2 alone (20 μM for 15 minutes) is used as positive control. (H). Quantification of blot in G. Arbitrary Densitometry Units (A.D.U.) ± SD were reported as pEGFR vs EGFR vs β-actin (n=3). (I) EGFR activation (Y845) after 24 h of **VA1213** treatment in MDA-MB-231. (J). Quantification of blot in G. Arbitrary Densitometry Units (A.D.U.) ± SD were reported as pEGFR vs β-actin (n=3). (K). Activation of pEGFR (Y845) in HT-29 pre-treated with **VA1213** (20 μM for 20 minutes) and then exposed to EGF (25 ng/ml for 3 minutes). (L). Quantification of blot in I. Arbitrary Densitometry Units (A.D.U.) ± SD were reported as pEGFR vs EGFR vs β-actin (n=3). ***$p \leq 0.001$ vs. ctr (untreated cells). (M). Activation of pEGFR (Y845) in MDA-MB-231 pre-treated with **VA1213** (20 μM for 20 minutes) and then exposed to EGF (25 ng/ml for 3 minutes). (N). Quantification of blot in K. Arbitrary Densitometry Units (A.D.U.) ± SD were reported as pEGFR vs EGFR vs β-actin (n=3). ***$p \leq 0.001$ vs. ctr (untreated cells).

4. Discussion

COX-2 may represent a valid target for antitumor pharmacotherapy [38], particularly in colorectal cancer in combination with antineoplastic therapies [1,13]. In this study, we demonstrated the *in vitro* efficacy and cellular mechanism of action of new selective COX-2 inhibitors, belonging to the family of vicinal diaryl-substituted heterocycles (VDHs) [25], comparing its activity to celecoxib, which has been widely tested for its antineoplastic properties [3, 34, 38].

These selective COX-2 inhibitors were previously characterized for their antinociceptive and anti-inflammatory properties, as well as their *in vitro* COX-2 inhibitory activity using J774 murine macrophages. Among them, **VA1213** exhibited the lowest *K*i value (0.008 μM; [28]), being significantly more potent than celecoxib (*K*i = 0.061 μM). Furthermore, **VA1213**, together with **VA692** and **VA694**, showed greater selectivity for COX-2 over COX-1 (COX-1 IC_{50} >10 μM), whereas celecoxib was significantly less selective (COX-1 IC_{50} >3.83 μM). Notably, **VA1213** displayed the highest COX-2 selectivity, with a COX-1/COX-2 selectivity index (SI) exceeding 1250 [28]. Among the COX-2 inhibitors, **VA1213** showed the highest efficacy both in reducing cell viability, with a peak effect at 48 h that persisted through 72 h, and in isolated enzyme. Its potency was comparable to celecoxib, which, in contrast, initiates its antiproliferative action as early as 24 h and sustains it over the same time frame. This suggests that celecoxib induces a rapid and sustained anti-proliferative effect, potentially through mechanisms that do not require prolonged cellular exposure or intracellular accumulation [40]. Indeed, the literature reports that celecoxib can trigger ROS production in carcinoma cells as early as 2 h [40] or rapidly enhances mitochondrial superoxide production in situ in cancer cells within minutes [41]. Additionally, celecoxib, but not other COX inhibitors, inhibits sarcoplasmic/ER calcium ATPase at micromolar concentrations, causing calcium leakage into the cytosol, ER stress, and apoptosis [42].

The ability of celecoxib to induce programmed cell death has been reported in the literature since the early 2000s. Arico and colleagues demonstrated that celecoxib induces apoptosis in HT-29 cells within the first 24 h of exposure, but only at high concentrations (50–100 μM). Importantly, a portion of HT-29 cells remained sensitive to celecoxib even in the presence of the caspase inhibitor, suggesting that celecoxib may also trigger caspase-independent cell death in these cells [43].

In contrast, **VA1213** exhibits maximal activity at 48 h, which remains stable up to 72 h, with IC50 values comparable to those of celecoxib. In the time-course experiments, celecoxib promoted a time-dependent accumulation of p21, with an initial rise at 6 h and, whereas **VA1213** exhibited an initial rise at 12 h and its maximal effect at 24 h. In contrast, the levels of cleaved caspase-3 did not follow a time-dependent pattern; instead, both compounds showed an increase after 12 h of treatment. This confirm that celecoxib may trigger cell death pathways that are at least partially caspase-independent [43], while p21, being a more general cell-cycle checkpoint regulator, displays a more temporally consistent response.

The data indicate that **VA694** exerts a more pronounced antiproliferative effect than its congener **VA692**, positioning itself between the more potent compounds **VA1213** and celecoxib, and the less active **VA692.** The contribution of NO release becomes more evident at higher concentrations in line with literature reports indicating that concentrations of at least 100 μM are required to elicit significant NO-mediated biological effects [44,45].

We tested the compounds on cell lines where COX-2 is known to play a critical role in tumor progression, such as colon cancer and breast cancer [46].

All compounds except celecoxib demonstrated greater toxicity against HT-29 cells and MCF-7, which express higher levels of COX-2, compared to triple-negative breast cancer cells MDA-MB-231 and colorectal cancer HCT-116 cell line. Furthermore, celecoxib exhibited

greater toxicity in these cells after just 24 h of treatment, a time frame inconsistent with cell death resulting solely from PGE2 synthesis inhibition.

The differing susceptibility of the cell lines to the tested compounds may be partly due to the presence of efflux pumps, which were not evaluated in this study.

Additionally, when dissecting the molecular mechanism triggered in the cells, we observed that at 20 μM, **VA1213** induced cell cycle arrest by increasing the proportion of cells in G0/G1 and reducing those in G2/M. A corresponding increase in the sub-G0/G1 population indicated enhanced cell death likely due to DNA fragmentation associated with apoptosis. Indeed, **VA1213** activated the apoptotic cascade by promoting caspase-3 cleavage in a manner consistent with COX-2 inhibition, and the associated reduction in arachidonic acid pathway products such as PGE2 (24 h) [47,48].

The mechanism of apoptosis induction by COX-2 inhibitors is widely debated and context dependent. Celecoxib is particularly known to have these COX-2-independent effects, which were reviewed by Ghosh et al [49]. These effects include the inhibition of β-catenin translocation to the nucleus, modulation of MAPK activation, blockade of AKT activation, regulation of 15-lipoxygenase-1 and 13-SHODE, induction of phosphodiesterases, activation of peroxisome proliferator-activated receptors, modulation of nuclear factor-kB activity, and induction of genes associated with nonsteroidal anti-inflammatory drugs [50].

Furthermore, we found dose-dependent impairment of ERK1/2 and AKT, which are critical for colon cancer cell growth and survival [35]. As ERK1/2 and AKT are downstream effectors of EGFR, which plays a crucial role in the development and progression of colorectal cancer, we examined EGFR phosphorylation and found reduced activation at tyrosine 845 (Y845). Importantly, this effect was not due to an off-target action of **VA1213**, as preincubation with the compound did not block EGF-induced receptor activation. The exact sequence of events will need to be elucidated in future studies. Indeed, these effects might instead stem from reduced PGE2 production and the consequent decrease in EP receptor signaling [51]. Our data substatiate this finding as exogenous PGE2 can rescue EGFR activation when COX-2 is inhibited by **VA1213**.

Previous studies have shown interplay between COX-2 and EGFR: COX-2-derived prostanoids can transactivate EGFR in colon cancer cells [52,53], whereas EGFR activation can stimulate COX-2 expression [54].

The molecular signaling, and functional studies here reported were conducted using a concentration of 20 μM for **VA1213** and an equimolar concentration of celecoxib as a control. Although the IC_{50} value of the test compound in MTT test at 24 h was 66.28 μM, we observed molecular modulations at 20 μM after 24 h of treatment. This is consistent with the notion that early signaling events and regulatory changes, particularly those involving cell cycle control, can occur at sub-cytotoxic concentrations and precede overt cell viability loss. This concentration and timing were deliberately chosen to avoid nonspecific toxicity and to capture early pharmacodynamic responses. Therefore, the observed alterations in key cell cycle regulators likely reflect direct pharmacodynamic effects of the compound rather than downstream consequences of cell death. The molecular data obtained at 24 h support the extent of cell death observed in the concentration–response curves at 48–72 h, where 20 μM **VA1213** induces detectable cytotoxicity, consistent with its subtoxic range given that IC_{50} values fall between 26 and 28 μM.

The progression of cancer cell migration, invasion and subsequent metastasis is the main cause of mortality in cancer patients [55]. Therefore, to evaluate the effect of **VA1213** and celecoxib on the migration of HT-29 cells, we performed a scratch assay. Following treatment of the cell with both COX-2 inhibitors, a clear reduction in cell migration was observed; however, at equal concentrations, **VA1213** demonstrated greater efficacy in

inhibiting migration. Finally, both COX-2 inhibitors showed comparable ability in reducing the clonogenic capacity of HT-29 cells.

Since the early 2000s, numerous studies have described the pharmacological effects both as a treatment and as prevention for many solid tumors, especially colorectal cancer, but also breast cancer [49,56,57]. Although efficacy has been proven in various clinical studies, the off-target effects of celecoxib have always raised concerns about the safety profile of these drugs [17,42,58]. Therefore, celecoxib is known for its ability to induce tumor-killing effects through COX-2-independent mechanisms in a range of cancer models [59].

In this context, the identification of COX-2 inhibitors, with greater selectivity, is an area of interest in antitumor pharmacology research.

This study presents several strengths. **VA1213** is a promising selective COX-2 inhibitor with interesting *in vitro* activity compared to celecoxib. Detailed molecular analyses revealed that **VA1213** induces apoptosis, impairs the activation of EGFR, ERK1/2, and AKT, and reduces both cell migration and clonogenic potential. Additionally, the direct comparison with celecoxib highlights **VA1213** as a potentially effective alternative. However, there are also limitations. All findings are based on *in vitro* models, and further *in vivo* and pharmacokinetic studies are required. Moreover, although **VA1213** appears selective, potential COX-2-independent effects should be explored to rule out unintended off-target actions.

In conclusion, these data demonstrate that pharmacological inhibition of COX-2 significantly increases tumor cell death and reduces their aggressiveness and metastatic potential. This effect is further supported by the impairment of several hallmarks involved in cancer progression. Among the COX-2 inhibitors here tested, **VA1213** emerged as the most potent, showing comparable activity to celecoxib, in line with its *in vitro* documented COX-2 selectivity.

Authors contribution: **Conceptualization:** Sandra Donnini, Lucia Morbidelli, Maurizio Anzini. **Methodology:** Sandra Donnini, Lucia Morbidelli, Maurizio Anzini, Valerio Ciccone. **Investigation:** Valerio Ciccone, Claudia Cecchin, Maria Frosini. **Formal analysis:** Valerio Ciccone, Claudia Cecchin, Maria Frosini. **Data curation:** Valerio Ciccone, Claudia Cecchin, Maria Frosini. **Resources:** Mario Saletti, Samuele Maramai, Germano Giuliani, Marco Paolino, Andrea Cappelli, Maurizio Anzini. **Project administration:** Lucia Morbidelli, Maurizio Anzini. **Supervision:** Lucia Morbidelli, Maurizio Anzini. **Writing – original draft:** Valerio Ciccone. **Writing – review and editing:** Sandra Donnini, Lucia Morbidelli, Maurizio Anzini, Valerio Ciccone, Claudia Cecchin, Maria Frosini, Mario Saletti, Samuele Maramai, Germano Giuliani, Marco Paolino, Andrea Cappelli.

Declaration of competing interest: The authors declare that they have no known competing financial interests or personal relationships that could have appeared to influence the work reported in this paper.

Data availability: The data underlying this article are available from the corresponding author upon reasonable request.

The authors declare that they agree to submit the article for publication.

5. References

1. Li S, Jiang M, Wang L, Yu S. Combined chemotherapy with cyclooxygenase-2 (COX-2) inhibitors in treating human cancers: Recent advancement. Biomedicine & Pharmacotherapy. 2020 Sept 1;129:110389.
2. Hashemi Goradel N, Najafi M, Salehi E, Farhood B, Mortezaee K. Cyclooxygenase-2 in cancer: A review. J Cell Physiol. 2019 May;234(5):5683–99.
3. Greenhough A, Smartt HJM, Moore AE, Roberts HR, Williams AC, Paraskeva C, et al. The COX-2/PGE2 pathway: key roles in the hallmarks of cancer and adaptation to the tumour microenvironment. Carcinogenesis. 2009 Mar;30(3):377–86.
4. Finetti F, Travelli C, Ercoli J, Colombo G, Buoso E, Trabalzini L. Prostaglandin E2 and Cancer: Insight into Tumor Progression and Immunity. Biology (Basel). 2020 Dec 1;9(12):434.
5. Bazzani L, Donnini S, Finetti F, Christofori G, Ziche M. PGE2/EP3/SRC signaling induces EGFR nuclear translocation and growth through EGFR ligands release in lung adenocarcinoma cells. Oncotarget. 2017 May 9;8(19):31270–87.
6. Sheehan KM, Sheahan K, O'Donoghue DP, MacSweeney F, Conroy RM, Fitzgerald DJ, et al. The Relationship Between Cyclooxygenase-2 Expression and Colorectal Cancer. JAMA. 1999 Oct 6;282(13):1254–7.
7. Liu Y, Sun H, Hu M, Zhang Y, Chen S, Tighe S, et al. The Role of Cyclooxygenase-2 in Colorectal Carcinogenesis. Clinical Colorectal Cancer. 2017 Sept 1;16(3):165–72.
8. Tsujii M, Kawano S, DuBois RN. Cyclooxygenase-2 expression in human colon cancer cells increases metastatic potential. Proceedings of the National Academy of Sciences. 1997 Apr;94(7):3336–40.
9. Mosalpuria K, Hall C, Krishnamurthy S, Lodhi A, Hallman DM, Baraniuk MS, et al. Cyclooxygenase-2 expression in non-metastatic triple-negative breast cancer patients. Mol Clin Oncol. 2014 Sept;2(5):845–50.
10. Sahu A, Raza K, Pradhan D, Jain AK, Verma S. Cyclooxygenase-2 as a therapeutic target against human breast cancer: A comprehensive review. WIREs Mechanisms of Disease. 2023;15(3):e1596.
11. Xu XC. COX-2 inhibitors in cancer treatment and prevention, a recent development. Anticancer Drugs. 2002 Feb;13(2):127–37.
12. Menter DG, Schilsky RL, DuBois RN. Cyclooxygenase-2 and Cancer Treatment: Understanding the Risk Should Be Worth the Reward. Clin Cancer Res. 2010 Mar 1;16(5):1384–90.
13. Pu D, Yin L, Huang L, Qin C, Zhou Y, Wu Q, et al. Cyclooxygenase-2 Inhibitor: A Potential Combination Strategy With Immunotherapy in Cancer. Front Oncol. 2021 Feb 26;11:637504.
14. Zappavigna S, Cossu AM, Grimaldi A, Bocchetti M, Ferraro GA, Nicoletti GF, et al. Anti-Inflammatory Drugs as Anticancer Agents. International Journal of Molecular Sciences. 2020 Jan;21(7):2605.
15. Ye SY, Li JY, Li TH, Song YX, Sun JX, Chen XW, et al. The Efficacy and Safety of Celecoxib in Addition to Standard Cancer Therapy: A Systematic Review and Meta-Analysis of Randomized Controlled Trials. Curr Oncol. 2022 Aug 25;29(9):6137–53.
16. Cotter J, Wooltorton E. New restrictions on celecoxib (Celebrex) use and the withdrawal of valdecoxib (Bextra). CMAJ. 2005 May 10;172(10):1299.
17. Gholizadeh E, Karbalaei R, Khaleghian A, Salimi M, Gilany K, Soliymani R, et al. Identification of Celecoxib-Targeted Proteins Using Label-Free Thermal Proteome Profiling on Rat Hippocampus. Mol Pharmacol. 2021 May 1;99(5):308–18.

18. Sun SX, Lee KY, Bertram CT, Goldstein JL. Withdrawal of COX-2 selective inhibitors rofecoxib and valdecoxib: impact on NSAID and gastroprotective drug prescribing and utilization. Curr Med Res Opin. 2007 Aug;23(8):1859–66.
19. Barmade MA, Ghuge RB. Chapter 1 - Vicinal Diaryl Heterocyclic System: A Privileged Scaffold in the Discovery of Potential Therapeutic Agents. In: Yadav MR, Murumkar PR, Ghuge RB, editors. Vicinal Diaryl Substituted Heterocycles [Internet]. Elsevier; 2018 [cited 2024 Sept 12]. p. 1–20. Available from: https://www.sciencedirect.com/science/article/pii/B9780081022375000018
20. Biava M, Porretta GC, Cappelli A, Vomero S, Manetti F, Botta M, et al. 1,5-Diarylpyrrole-3-acetic acids and esters as novel classes of potent and highly selective cyclooxygenase-2 inhibitors. J Med Chem. 2005 May 5;48(9):3428–32.
21. Anzini M, Rovini M, Cappelli A, Vomero S, Manetti F, Botta M, et al. Synthesis, biological evaluation, and enzyme docking simulations of 1,5-diarylpyrrole-3-alkoxyethyl ethers as selective cyclooxygenase-2 inhibitors endowed with anti-inflammatory and antinociceptive activity. J Med Chem. 2008 Aug 14;51(15):4476–81.
22. Di Capua A, Sticozzi C, Brogi S, Brindisi M, Cappelli A, Sautebin L, et al. Synthesis and biological evaluation of fluorinated 1,5-diarylpyrrole-3-alkoxyethyl ether derivatives as selective COX-2 inhibitors endowed with anti-inflammatory activity. Eur J Med Chem. 2016 Feb 15;109:99–106.
23. Reale A, Brogi S, Chelini A, Paolino M, Di Capua A, Giuliani G, et al. Synthesis, biological evaluation and molecular modeling of novel selective COX-2 inhibitors: sulfide, sulfoxide, and sulfone derivatives of 1,5-diarylpyrrol-3-substituted scaffold. Bioorganic & Medicinal Chemistry. 2019 Oct 1;27(19):115045.
24. Biava M, Porretta GC, Poce G, Battilocchio C, Alfonso S, Rovini M, et al. Novel analgesic/anti-inflammatory agents: diarylpyrrole acetic esters endowed with nitric oxide releasing properties. J Med Chem. 2011 Nov 24;54(22):7759–71.
25. Anzini M, Di Capua A, Valenti S, Brogi S, Rovini M, Giuliani G, et al. Novel analgesic/anti-inflammatory agents: 1,5-diarylpyrrole nitrooxyalkyl ethers and related compounds as cyclooxygenase-2 inhibiting nitric oxide donors. J Med Chem. 2013 Apr 25;56(8):3191–206.
26. Martelli A, Testai L, Anzini M, Cappelli A, Di Capua A, Biava M, et al. The novel anti-inflammatory agent VA694, endowed with both NO-releasing and COX2-selective inhibiting properties, exhibits NO-mediated positive effects on blood pressure, coronary flow and endothelium in an experimental model of hypertension and endothelial dysfunction. Pharmacol Res. 2013 Dec;78:1–9.
27. Cheleschi S, Calamia V, Fernandez-Moreno M, Biava M, Giordani A, Fioravanti A, et al. In vitro comprehensive analysis of VA692 a new chemical entity for the treatment of osteoarthritis. Int Immunopharmacol. 2018 Nov;64:86–100.
28. Saletti M, Maramai S, Reale A, Paolino M, Brogi S, Di Capua A, et al. Novel analgesic/anti-inflammatory agents: 1,5-Diarylpyrrole nitrooxyethyl sulfides and related compounds as Cyclooxygenase-2 inhibitors containing a nitric oxide donor moiety endowed with vasorelaxant properties. Eur J Med Chem. 2022 Nov 5;241:114615.
29. Ciccone V, Simonis V, Del Gaudio C, Cucini C, Ziche M, Morbidelli L, et al. ALDH1A1 confers resistance to RAF/MEK inhibitors in melanoma cells by maintaining stemness phenotype and activating PI3K/AKT signaling. Biochem Pharmacol. 2024 June;224:116252.
30. Filippelli A, Ciccone V, Del Gaudio C, Simonis V, Frosini M, Tusa I, et al. ERK5 mediates pro-tumorigenic phenotype in non-small lung cancer cells induced by PGE2. Biochimica et Biophysica Acta (BBA) - Molecular Cell Research. 2024 Oct 1;1871(7):119810.

31. Ciccone V, Terzuoli E, Ristori E, Filippelli A, Ziche M, Morbidelli L, et al. ALDH1A1 overexpression in melanoma cells promotes tumor angiogenesis by activating the IL-8/Notch signaling cascade. International Journal of Molecular Medicine. 2022 July 1;50(1):1–17.
32. Ciccone V, Filippelli A, Bacchella C, Monzani E, Morbidelli L. The Nitric Oxide Donor [Zn(PipNONO)Cl] Exhibits Antitumor Activity through Inhibition of Epithelial and Endothelial Mesenchymal Transitions. Cancers. 2022 Jan;14(17):4240.
33. Park JY, Pillinger MH, Abramson SB. Prostaglandin E2 synthesis and secretion: the role of PGE2 synthases. Clin Immunol. 2006 June;119(3):229–40.
34. He C xi, Ai J, Xing W qiang, Chen Y, Zhang H tian, Huang M, et al. Yhhu3813 is a novel selective inhibitor of c-Met Kinase that inhibits c-Met-dependent neoplastic phenotypes of human cancer cells. Acta Pharmacol Sin. 2014 Jan;35(1):89–97.
35. Koveitypour Z, Panahi F, Vakilian M, Peymani M, Seyed Forootan F, Nasr Esfahani MH, et al. Signaling pathways involved in colorectal cancer progression. Cell & Bioscience. 2019 Dec 2;9(1):97.
36. Han YS, Lee JH, Lee SH. Fucoidan inhibits the migration and proliferation of HT-29 human colon cancer cells via the phosphoinositide-3 kinase/Akt/mechanistic target of rapamycin pathways. Mol Med Rep. 2015 Sept;12(3):3446–52.
37. Wang C, Chen Y, Wang Y, Liu X, Liu Y, Li Y, et al. Inhibition of COX-2, mPGES-1 and CYP4A by isoliquiritigenin blocks the angiogenic Akt signaling in glioma through ceRNA effect of miR-194-5p and lncRNA NEAT1. J Exp Clin Cancer Res. 2019 Aug 22;38(1):371.
38. Sarkar FH, Adsule S, Li Y, Padhye S. Back to the future: COX-2 inhibitors for chemoprevention and cancer therapy. Mini Rev Med Chem. 2007 June;7(6):599–608.
39. Huang S, Sinicrope FA. Celecoxib-induced apoptosis is enhanced by ABT-737 and by inhibition of autophagy in human colorectal cancer cells. Autophagy. 2010 Feb;6(2):256–69.
40. Zhu J, May S, Ulrich C, Stockfleth E, Eberle J. High ROS Production by Celecoxib and Enhanced Sensitivity for Death Ligand-Induced Apoptosis in Cutaneous SCC Cell Lines. Int J Mol Sci. 2021 Mar 31;22(7):3622.
41. Pritchard R, Rodríguez-Enríquez S, Pacheco-Velázquez SC, Bortnik V, Moreno-Sánchez R, Ralph S. Celecoxib inhibits mitochondrial O2 consumption, promoting ROS dependent death of murine and human metastatic cancer cells via the apoptotic signalling pathway. Biochem Pharmacol. 2018 Aug;154:318–34.
42. Gong L, Thorn CF, Bertagnolli MM, Grosser T, Altman RB, Klein TE. Celecoxib pathways: pharmacokinetics and pharmacodynamics. Pharmacogenet Genomics. 2012 Apr;22(4):310–8.
43. Arico S, Pattingre S, Bauvy C, Gane P, Barbat A, Codogno P, et al. Celecoxib induces apoptosis by inhibiting 3-phosphoinositide-dependent protein kinase-1 activity in the human colon cancer HT-29 cell line. J Biol Chem. 2002 Aug 2;277(31):27613–21.
44. Waheed S, Cheng RY, Casablanca Y, Maxwell GL, Wink DA, Syed V. Nitric Oxide Donor DETA/NO Inhibits the Growth of Endometrial Cancer Cells by Upregulating the Expression of RASSF1 and CDKN1A. Molecules. 2019 Oct 16;24(20):3722.
45. Ciccone V, Monti M, Monzani E, Casella L, Morbidelli L. The metal-nonoate Ni(SalPipNONO) inhibits in vitro tumor growth, invasiveness and angiogenesis. Oncotarget. 2018 Jan 30;9(17):13353–65.
46. Gargano A, Greco I, Lupia C, Alcaro S, Ambrosio FA. Rosmarinus officinalis L. as Fascinating Source of Potential Anticancer Agents Targeting Aromatase and COX-2: An Overview. Molecules. 2025 Apr 12;30(8):1733.

47. Cai F, Chen M, Zha D, Zhang P, Zhang X, Cao N, et al. Curcumol potentiates celecoxib-induced growth inhibition and apoptosis in human non-small cell lung cancer. Oncotarget. 2017 Dec 14;8(70):115526–45.
48. Zhu X, Zhou M, Liu G, Huang X, He W, Gou X, et al. Autophagy activated by the c-Jun N-terminal kinase-mediated pathway protects human prostate cancer PC3 cells from celecoxib-induced apoptosis. Experimental and Therapeutic Medicine. 2017 May 1;13(5):2348–54.
49. Ghosh N, Chaki R, Mandal V, Mandal SC. COX-2 as a target for cancer chemotherapy. Pharmacol Rep. 2010 Mar 1;62(2):233–44.
50. Gee J, Lee IL, Jendiroba D, Fischer SM, Grossman HB, Sabichi AL. Selective cyclooxygenase-2 inhibitors inhibit growth and induce apoptosis of bladder cancer. Oncol Rep. 2006 Feb;15(2):471–7.
51. Nakanishi M, Rosenberg DW. Multifaceted roles of PGE2 in inflammation and cancer. Semin Immunopathol. 2013 Mar;35(2):123–37.
52. Pai R, Soreghan B, Szabo IL, Pavelka M, Baatar D, Tarnawski AS. Prostaglandin E2 transactivates EGF receptor: A novel mechanism for promoting colon cancer growth and gastrointestinal hypertrophy. Nat Med. 2002 Mar;8(3):289–93.
53. Donnini S, Finetti F, Solito R, Terzuoli E, Sacchetti A, Morbidelli L, et al. EP2 prostanoid receptor promotes squamous cell carcinoma growth through epidermal growth factor receptor transactivation and iNOS and ERK1/2 pathways. FASEB J. 2007 Aug;21(10):2418–30.
54. Patrignani P, Dovizio M. COX-2 and EGFR: Partners in Crime Split by Aspirin. EBioMedicine. 2015 May;2(5):372–3.
55. Shin AE, Giancotti FG, Rustgi AK. Metastatic colorectal cancer: mechanisms and emerging therapeutics. Trends Pharmacol Sci. 2023 Apr;44(4):222–36.
56. Brown JR, DuBois RN. COX-2: a molecular target for colorectal cancer prevention. J Clin Oncol. 2005 Apr 20;23(12):2840–55.
57. Wang D, DuBois RN. Role of prostanoids in gastrointestinal cancer. J Clin Invest. 2018 July 2;128(7):2732–42.
58. Matheny RW, Kolb AL, Geddis AV, Roberts BM. Celecoxib impairs primary human myoblast proliferation and differentiation independent of cyclooxygenase 2 inhibition. Physiol Rep. 2022 Nov 2;10(21):e15481.
59. Patel MI, Subbaramaiah K, Du B, Chang M, Yang P, Newman RA, et al. Celecoxib inhibits prostate cancer growth: evidence of a cyclooxygenase-2-independent mechanism. Clin Cancer Res. 2005 Mar 1;11(5):1999–2007.